Electronic Effects in CO Chemisorption on Pt−Pb Intermetallic Surfaces: A Theoretical Study

Chinmoy Ranjan, Roald Hoffmann,* Francis J. DiSalvo, and Héctor D. Abruña

Department of Chemistry and Chemical Biology, Cornell University, Ithaca, New York 14853

Received: June 15, 2007; In Final Form: August 28, 2007

The chemisorption of CO on surfaces of Pt−Pb intermetallic compounds, found to be useful as fuel cell electrocatalysts, was analyzed theoretically. Specifically, density-functional theory and extended Hückel-based calculations on CO adsorption on Pt(111), Pt_3Pb(111), and PtPb(0001) surfaces are reported. Binding energies on Pt_3Pb(111) are computed to be generally smaller than binding energies on Pt(111). The binding energies at the 2- and 3-fold sites on Pt_3Pb(111) increase if there is a Pb atom underneath the site in the second surface layer. The binding energies on PtPb(0001) are much higher than those on the other surfaces. These trends have been analyzed with crystal overlap Hamilton population (COHP)-based energy partitioning. The most stabilizing interaction in chemisorption is the Pt−adsorbate bond formation; the surface and the adsorbate are internally destabilized. The major surface effects are pretty much restricted to the top two layers. The binding energy trend for the top site chemisorption follows the Pt−adsorbate interaction term (most stabilizing interaction term in chemisorption). This surface Pt−adsorbate interaction term, for top site chemisorption, has been analyzed further with a Frontier molecular orbital formalism based on the extended Hückel calculations. Electron donation from Pb atoms to Pt atoms plays an important role in distinguishing chemisorption on these surfaces. The higher Fermi energy of the Pt−Pb intermetallic surfaces, relative to Pt(111) surface, leads to a weaker Pt−adsorbate interaction, which correlates well with the lower binding energy on Pt−Pb intermetallic surfaces when compared to Pt(111). The variation of the binding energy within the 2- and 3-fold sites on Pt_3Pb(111) cannot be explained by the Pt−adsorbate interaction term alone. From a detailed COHP analysis of the surface and adsorbate, we find that the adsorption site affects the electron movements (transfer of electrons) in the surface slab upon chemisorption and through them the overall binding energy of the adsorbate. The difference in binding energies between the Pt_3Pb(111) hcp and fcc sites can be explained this way.

1. Introduction

The materials used as electrocatalysts in near ambient temperature hydrogen/oxygen fuel cells have remained virtually unchanged since the invention of the fuel cell by Sir William Grove in 1839.[1] Even today both the anode and the cathode are made of platinum. Although Pt has a very high activity toward hydrogen oxidation, it is greatly reduced if even small amounts of CO (ppm), sulfides (ppb), and other surface poisons are present in the hydrogen fuel stream. Other fuels being studied for use in near ambient temperature fuel cells are formic acid and methanol. Formic acid is frequently used as a screening agent for checking the propensity of the anode catalysts to be poisoned by CO.[2] CO may be present in hydrogen as an impurity or as an intermediate in the oxidation of carbon-containing fuels.

CO poisoning can be somewhat mitigated by alloying Pt with Ru.[3,4] CO oxidation to CO_2 is believed to be easier on PtRu alloy surfaces, where Ru sites are deemed to be important, acting as sites for nucleation of OH species that provide the oxygen necessary for CO oxidation.[4] However PtRu alloy surfaces are not stable due to its low energy of formation from the constituent metals.[2] The Ru tends to segregate into the bulk with time, resulting in a Pt-enriched surface and diminished catalytic activity, especially in the presence of CO. In contrast, ordered intermetallic compounds with a high energy of formation from the constituent elements tend to form more stable surfaces that are compositionally stable under the operating electrochemical conditions.[2]

Several ordered intermetallic compounds have been identified as a new class of anode catalysts that are resistant to CO poisoning under electrochemical conditions.[2] The nature of these catalytic surfaces, like most heterogeneous catalytic surfaces, is not well-known. Also, experimental techniques to evaluate them are not well developed. In such a situation, it becomes important to explore the behavior of these catalysts and to learn about them theoretically as much as possible. PtPb has been one of the most active systems of these binary intermetallic compounds.[2]

PtPb was recently shown to be resistant to CO poisoning when formic acid is used as a fuel,[2] whereas a pure Pt surface poisons immediately. Further, PtPb is much more resistant to sulfur poisoning than Pt or Pt alloys.[2] Where does the resistance come from? One possibility is that CO does not bind (or binds very weakly when compared to pure Pt) to a PtPb surface. It is also conceivable that CO is formed during the oxidation of formic acid but is easily removed from the surface. Another possibility is that formic acid can be oxidized on PtPb in pathways that do not involve the formation of CO. As a reviewer remarked, it is very difficult to predict the correct surface structure in these catalytic systems, especially under electro-

* To whom correspondence should be addressed. Email: rh34@cornell.edu. Tel: 607-255-3419.

10.1021/jp0746603 CCC: $37.00
Published on Web 11/01/2007

chemical conditions. In the absence of any specific knowledge about these catalytic surfaces, we theoretically investigate single crystalline and pristine surfaces to search for clues for the above differences.

Our aim in this paper is to theoretically explore chemisorption of catalytically important molecules such as CO on the surface of intermetallic materials made from Pt and Pb and to compare them to chemisorption on Pt. Specifically, we carry out plane-wave density-functional theory (DFT) and extended Hückel[5−8] calculations on CO chemisorption on Pt(111), Pt_3Pb(111), and Pt-terminated PtPb(0001) surfaces and establish a model for chemisorption on them. The Pt_3Pb(111) surface provides, along with new adsorption sites, an avenue for exploring the electronic effects of adding Pb atoms to the Pt structure. PtPb(0001), in contrast, provides a way to explore a similar hexagonal surface, but one not close packed like Pt(111) and Pt_3Pb(111). The Pt−Pt distance (4.39 Å) in PtPb(0001) is much larger than that found on Pt(111) or Pt_3Pb(111) (∼ 2.8 Å).

PtPb and Pt_3Pb are some of the simple binary intermetallic compounds that can act as model systems for understanding the effects of the presence of two different types of atoms on the surface and in the bulk. This study will systematically explore the extent to which the bulk electronic structures of these intermetallic compounds influence the adsorption of small molecules on these surfaces.

The paper's work may be roughly divided into four parts. In the first section, we look at the bulk structures of the pure Pt and Pt−Pb intermetallic compounds. This is followed with a discussion of the electronic structures of these solids by use of extended Hückel calculations.

The second section contains calculations of CO chemisorption on the Pt(111), Pt_3Pb(111), and PtPb(0001) intermetallic surfaces. The geometry and energetics of chemisorption are discussed, and specific trends pertaining to intermetallic surfaces are extracted from these calculations.

In the third section, we discuss the crystal overlap Hamilton population (COHP) method, an analytical tool for understanding the observed chemisorption trends.

In the fourth section, we apply the COHP method to analyze certain chemisorption trends obtained from DFT calculations. We end this section with a FMO analysis of the chemisorption at the top sites of these surfaces.

2. Computational Methodology and Calculations on the Bulk Structures

Generalized gradient-corrected DFT[9−12] periodic calculations, as implemented in the Vienna ab initio simulation package,[13−18] were carried out to model the bulk structures. Specifically, a GGA-PAW plane-wave basis with an energy cutoff of 400 eV was used to model all bulk structures. Same methodology is again used later in the paper to model chemisorption on various surfaces.

With a desire to connect between bulk electronic properties and surface adsorption, we start with the theoretical evaluation of bulk structures of Pt, Pt_3Pb, and PtPb. Figure 1 shows the unit cells of the bulk structure and the DFT optimized lattice parameters (which are within 2% of experimentally observed values). Replacing one of the four Pt atoms (the corner atom) of the fcc crystal (space group $Fm\bar{3}m$) by a Pb atom leads to the primitive cubic cell of Pt_3Pb (space group $Pm\bar{3}m$). The calculated Pt−Pt distance in Pt_3Pb is increased to 2.93 from 2.82 Å in pure Pt metal; the Pt−Pb distance is 2.93 Å. The Pt and Pt_3Pb structures may also be described by stacking of close-packed (111) planes in an ABCABC... pattern. Each Pt atom

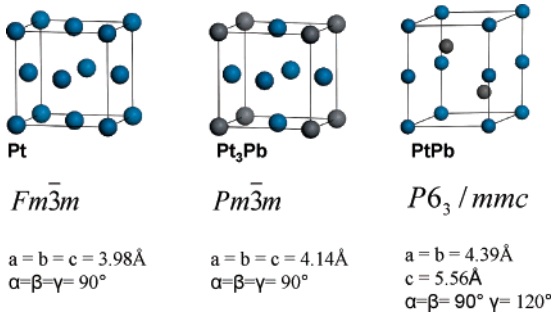

Figure 1. The unit cells of Pt, Pt_3Pb, and PtPb. The Pt atoms are blue and Pb atoms are black.

in the Pt metal has 12 nearest neighbor (NN) Pt atoms. In Pt_3-Pb, each Pb atom has 12 NN Pt atoms in a similar coordination and each Pt atom has 8 NN Pt atoms in a tetragonal coordination pattern and 4 NN Pb atoms in a square-planar coordination.

PtPb crystallizes in the NiAs structure (space group $P6_3/mmc$). The structure can be described as one in which the Pt atoms form hexagonal layers (not close packed, as the Pt−Pt distance is 4.39 Å) stacked in an "eclipsed" hexagonal way. Pb atoms occupy alternate interstitial positions over each Pt layer in a stacking sequence described as AbAcAbAc..., where Pt forms the A layers and Pb occupies the b and c positions. Thus the Pb atoms also form hexagonal layers. Both Pt and Pb are six-coordinate; the 6 NN of Pt are Pb atoms, forming a trigonal antiprismatic or distorted octahedral coordination environment. Pb is coordinated by the six nearest neighbor Pt atoms in a trigonal prismatic arrangement. The closest Pt−Pt, Pb−Pb, and Pt−Pb separations are 2.78, 3.76, and 2.89 Å, respectively. The distances reported in the paper are theoretically computed values, which as we mentioned earlier match well with experimental bulk separations.

Because of our limitations with analyzing bonding with the available plane-wave-based code and our limited computational resources, we use the far less computationally expensive extended Hückel (eH) method to analyze bonding in this study. The eH parameters for Pt and Pb have been adjusted to give reasonable agreement with band structures and DOS obtained from DFT calculations of the bulk structures (more details can be found in the Appendix). Further analysis of the bonding was carried out with the crystal overlap Hamilton population[19,20] (COHP) scheme introduced by Blöchl and Dronskowski. The COHP analysis can be described as an energy-weighted overlap population analysis for periodic solids or alternatively as an energy partitioning scheme. All calculations were converged with respect to the number of k-points, and the results are reported from calculations done with a similar density of k-points in the reciprocal space (1000 k-points for Pt and Pt_3-Pb and 567 k-points for PtPb over the entire Brillouin zone).

3. Bonding in Bulk Intermetallics

All compounds are computed to be metallic (as expected). The densities of states (DOS, Figure 2) show that with increasing atom percent of Pb, the Pt d bands (bands between −9 and −15 eV) become increasingly less dispersed and, on average, move further down below the Fermi energy, as one goes from Pt to Pt_3Pb to PtPb. The source of the Pt d bandwidth is primarily in the Pt−Pt contacts. The number of such contacts goes down from 12 in Pt metal to 8 in Pt_3Pb and 2 in PtPb.

The DOS for Pt_3Pb has a pseudogap (a deep minimum in the DOS) at the Fermi level. Sublattice calculations on Pt_3Pb (Figure 3(top)) reveal that removal of one Pt atom from the fcc unit cell of pure Pt (in addition to slightly expanding the lattice

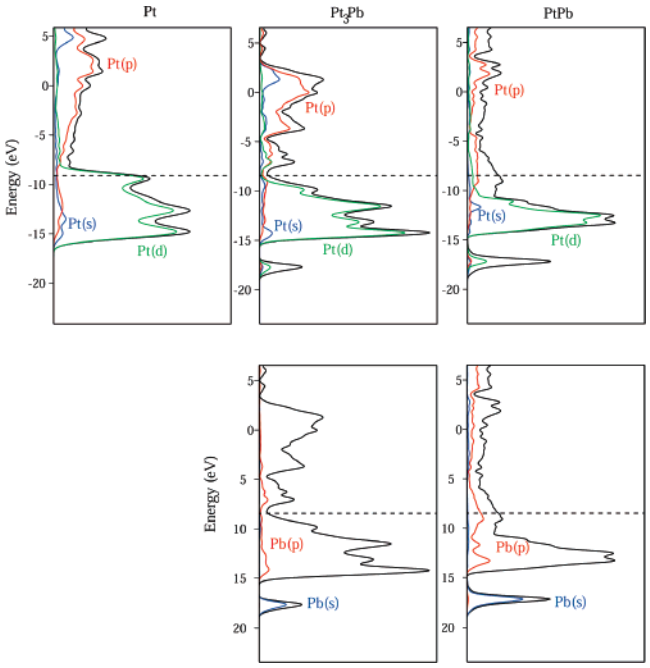

Figure 2. The Pt and Pb contributions (s in blue, p in red, and d in green) to the DOS in Pt, Pt_3Pb, and PtPb. The Fermi level is shown with dashed lines.

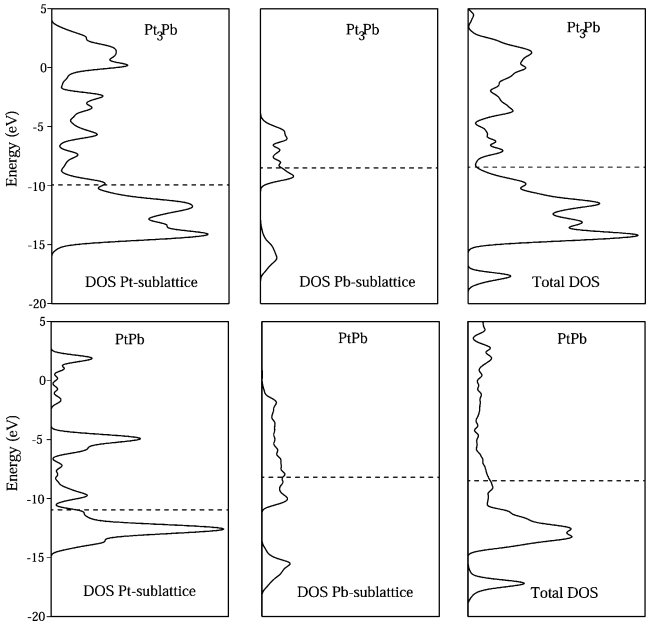

Figure 3. The DOS obtained from sublattice calculations on Pt_3Pb (top) and PtPb (bottom). The Fermi level is shown with dashed lines.

parameters from 3.98 to 4.14 Å) is almost enough to create this pseudogap. The insertion of a Pb atom in the empty site leads to Pt−Pb bonding and stabilization of the Pt lattice (Figure 3 (top), COHP calculations shown in Figure 4 and Table 1). Most of the Pb s levels are pushed down in energy due to the Pt−Pb interaction. There is also some electron transfer from Pb to the Pt sublattice, which finally establishes the Fermi energy at the pseudogap. The total DOS of Pt_3Pb retains most features of the Pt sublattice (with a higher Fermi level).

The Pt sublattice in PtPb is formed of chains of Pt atoms (Pt−Pt 2.78 Å) running parallel to each other (Figure 1). The chains are separated by 4.39 Å. This distance is much larger than the bonding distance for Pt atoms (∼2.80 Å in the Pt metal). The sharp features (singularities) of the DOS (Figure 2) essentially indicate the undercoordinated nature of Pt atoms in the Pt chain (CN = 2). The Pb sublattice interacts strongly with the Pt sublattice (Figure 3, COHP calculations in Figure 4 and Table 1), removing most of the singularities. The peak due to Pt d bands (around −12.5 eV) is pretty much retained in the total DOS of PtPb, due to the compact nature of the d orbitals compared to Pt s and p. As mentioned earlier, the d bandwidth, as it is, essentially originates from d(Pt)−d(Pt) interactions along the *c* axis.

Pt d orbitals dominate the region around the Fermi energy for Pt metal. There is a very small electronic density of states at the Fermi energy for Pt_3Pb due to the aforementioned pseudogap. In PtPb, the Pt and Pb p states are populated more than the Pt s,d states around the Fermi energy. Pb s states are more dispersed in PtPb than in Pt_3Pb.

A molecule (such as CO) coming onto the surface of these materials brings along filled donor and empty acceptor levels. From a frontier orbital perspective,[21] these levels would interact most effectively with those surface states close to them in energy and which overlap effectively. Thus, in thinking about chemisorption and reactivity, one is led to focus on such levels of the intermetallic compounds near the Fermi level. Given the lower position of the 5d levels, one could speculate that in PtPb and Pt_3Pb, the importance of Pt d levels toward binding an adsorbate is diminished relative to the s and p orbitals, compared to Pt metal. The adsorption at Pb sites would be dominated by interaction with the Pb p levels (dispersed around the Fermi level region), as the Pb s levels remain far below the Fermi energy.

The COHP curves (Figure 4) show the familiar bonding (negative COHP) and antibonding type interactions for the Pt−Pt interaction in Pt metal. The bonding states are more bonding than the antibonding states are antibonding due to the mixing of the Pt−Pt s,p bonding levels into the d−d antibonding levels.[21] We see the remnant of this interaction in both Pt_3Pb and PtPb.

States around the Fermi level in Pt metal are Pt−Pt antibonding in nature. In PtPb, these states are Pt−Pt antibonding but Pt−Pb and Pb−Pb bonding. In Pt_3Pb, the states around the Fermi level are mostly nonbonding in character.

In Pb-containing solids the Pt−Pb bonds are the strongest bonds in the structure; this is supported by the higher values of the Pt−Pb integrated COHP compared to those of other types of bonds (Table 1) in these phases.

4. The Surfaces of Intermetallics

We have carried out slab calculations to model the various surfaces. Two-dimensional slabs were thus constructed in a three-dimensional setting by inserting a vacuum layer of ∼10 Å between the slabs, each made up of four atomic layers. In the calculations, only the geometry of the top layer of each slab was relaxed. DFT methodology described in section 2 was also used to model the surfaces. In addition a (4 × 4 × 1) set of Monkhorst pack grid of k-points was used.[22] The surface unit cell sizes were chosen so as to have a low adsorbate coverage (0.25); this assures that all the adsorbates stay out of van der Waals contact with each other.

The surfaces calculated are shown in Figure 5. Pt(111) is a close-packed surface with a computed Pt−Pt distance of 2.82 Å. There are, in principle, four different sites available for chemisorption: Pt on-top (A), a 2-fold bridge site (B), and two 3-fold sites (fcc C(1), hcp C(2)). The $Pt_3Pb(111)$ surface is similar and has a Pt−Pt and Pt−Pb distance of 2.93 Å each.

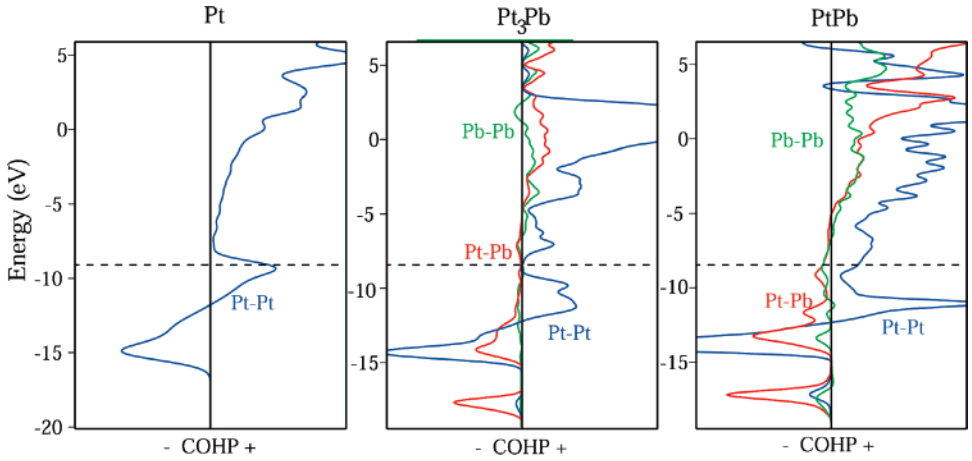

Figure 4. COHP plots for Pt−Pt, Pt−Pb, and Pb−Pb bonding in Pt metal, Pt_3Pb, and PtPb, respectively. Negative values on the horizontal axes imply bonding interaction. Fermi levels, aligned for comparison, are shown as dashed lines.

TABLE 1: The Integrated-COHP (eV) Values for Various Contacts in the Pt, Pt_3Pb, and PtPb

contacts	Pt metal	Pt_3Pb	PtPb
Pt−Pt	−2.14	−1.66	−2.62
Pt−Pb		−3.31	−5.19
Pb−Pb			−0.98

TABLE 2: CO Adsorption on Pt(111), Pt_3Pb(111), and PtPb(0001) Surfaces[a]

surfaces	sites	binding energies (eV)	(Pt/Pb)−C distance (Å)	C−O distance (Å)
Pt(111)	A (on-top)	−1.59	1.85	1.16
	B (bridge)	−1.71	2.03	1.18
	C(1) (fcc)	−1.74	2.11	1.19
	C(2) (hcp)	−1.76	2.11	1.19
Pt_3Pb(111)	A′ (on-top)	−1.22	1.87	1.16
	B′(1) (bridge1)	−0.99	2.05	1.18
	B′(2) (bridge2)	−1.43	2.05	1.19
	C′(1) (fcc)	−1.19	2.11	1.20
	C′(2) (hcp)	−1.62	2.13	1.20
PtPb(0001)	A″ (on-top)	−2.07	1.86	1.16

[a] The optimization is constrained to top surface layer and the adsorbate. Relaxation is performed only along the surface normal. The adsorption sites are shown in Figure 5.

Besides the Pb sites (on top and bridging with another Pt), additional sites are introduced on the Pt atoms in Pt_3Pb(111). If one considers the top two surface layers, then among the 3-fold sites, the fcc site on Pt(111) (C(1)) is similar to the fcc site (C′1) on Pt_3Pb(111). Both have Pt atoms in the top and the second (subsurface) layers. The hcp sites differ, with Pt_3Pb-(111) having a Pb atom in the subsurface layer directly underneath the adsorption site (C′(2)). Similarly, there is an additional 2-fold site (B′(2)) on Pt_3Pb(111) that has a Pb atom in the subsurface layer with Pt atoms forming the top layer.

The PtPb(0001) surface can be either Pt or Pb terminated, as Pt and Pb form alternating layers. We calculated the Pt-terminated surface, since surface Pt sites are considered to be important for catalysis. The Pt−Pt computed distance is 4.39 Å. The size of the (2 × 2) unit cell is much larger. We maintain the surface Pt coverage at 0.25. The wide spacing of Pt atoms allows the Pb atoms in the second layer to be exposed to attack by adsorbates, leading to two kinds of sites: Pt on top and Pb on top. The surface Pt on this surface is less coordinated (CN = 4, only to the subsurface Pb and Pt) than the surface Pt on Pt(111) or Pt_3Pb(111) (CN = 9).

5. CO Molecule Chemisorption

In our study, geometry optimizations are restricted to the top surface layer and adsorbate atoms, which are relaxed only along the surface normal. Binding energies (BEs) have been calculated with the following formula:

$$\text{BE} = \text{Total energy of surface with adsorbate bound on it} - \text{Energy of clean surface (optimized)} - \text{Energy of the H atom (not interacting with the surface)} \quad (1)$$

Binding energies and important geometrical parameters obtained from calculations for the three surfaces for CO chemisorption are reported in Table 2. The adsorption sites are described in Figure 5.

From our calculations on Pt(111), CO binds the strongest in the 3-fold sites. The binding energy and bond distance values are close to the theoretical and experimental values reported in the literature.[23−25] Experimentally, Ogletree et al. reported a CO bond distance of 1.15 ± 0.05 Å and a Pt−C bond distance of 1.85 ± 0.1 Å for the on-top site in their experiments.[25] It is known that the site selectivity for CO on Pt(111) is not well reproduced by DFT calculations in general.[26] Experiments suggest that the Pt on-top site is most stable,[23] whereas DFT calculations show a preference for the 3-fold hcp site as the most stable one.[24] In this study, we shall try to focus on differences between the surfaces rather than small energy differences between the various sites. Our goal here is to identify trends arising out of the calculations and analyze the electronic effect of the Pb atoms.

In Figure 6, we compare the BEs at various sites on the three different surfaces. The BEs on Pt_3Pb(111) are lower than the values obtained for comparable sites on Pt(111). The BE on PtPb(0001) for Pt on-top site is much higher than those on the other two surfaces. The sites that have Pb atoms in the second layer underneath the Pt (B′(2) and C′(2)) bind CO more strongly compared to those which do not have Pb atoms underneath (B′-(1) and C′(1)). Comparable trends have been observed in DFT calculations by Shubina et al. for the Pt_3Sn(111) surface.[27] In comparison to Pt_3Pb(111), both the 3-fold sites on Pt(111) have similar binding energies (within ±0.02 eV).

CO does not bind to the Pb sites on any surface, as expected (CO usually does not bind to main group elements). From Figure 6 one can infer two things: first, the BEs for CO are in general lower for the Pt_3Pb(111) surface compared to those for Pt(111); second, the presence of Pb atoms in the second layer underneath Pt atoms enhances the binding energies at certain sites. The

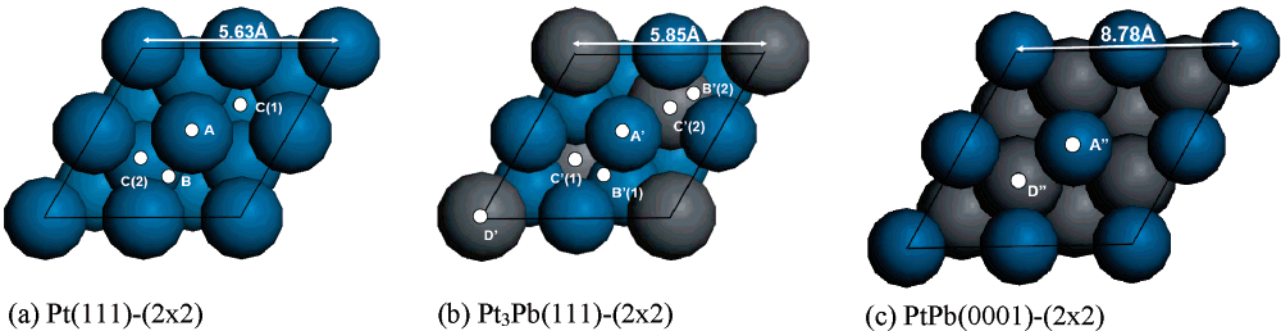

Figure 5. Various (2 × 2) surfaces indicating the adsorption sites (A = on-top sites on Pt atoms, B = bridge sites on Pt atoms, C = 3-fold sites on Pt atoms, and D = on-top sites on Pb atoms on various surfaces). Where several sites exist, numbers are used to distinguish them. Primes are used to distinguish between similar sites on different surfaces (single prime = $Pt_3Pb(111)$; double prime = PtPb(0001)) The lattice parameters of the (2 × 2) surface cells are indicated (white). Pt and Pb atoms are blue and gray, respectively.

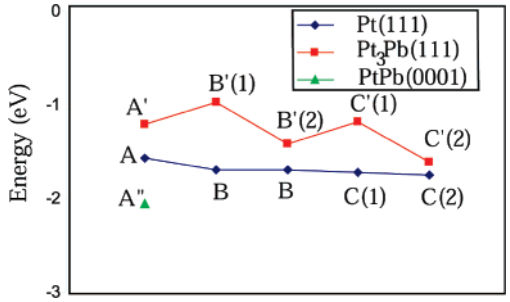

Figure 6. Binding energies for CO adsorption on Pt atoms on all the surfaces (color coded). Similar sites, as described in Table 2, have been placed at same points along the *x* axis for comparison (i.e., A, A′, A″ are all Pt on-top sites).

same phenomenon was also observed in case of H atom chemisorption, shown in section 1 of Supporting Information. The difference between the BEs of H on the Pt(111) and Pt_3-Pb(111) surfaces is smaller than the difference observed for CO on these surfaces. In the case of H adsorption, the enhancement effect of the Pb atom in these sites makes H bind to the Pt_3-Pb(111) surface even more strongly than on to the Pt(111) surface.

As the Pb atoms on the $Pt_3Pb(111)$ and PtPb(0001) surfaces remain free from CO, one can speculate that in an electrochemical environment Pb sites can act as places that nucleate oxygen-containing species like OH and O from water and aid with oxidative removal of CO bound on Pt sites. Proving such a mechanism would require a more detailed knowledge of these surfaces. In this paper, we would just focus on explaining the various trends seen in surface chemisorption.

6. Adsorption Studies Using Extended Hückel-Based Methods

In our bid to understand the electronic effects in chemisorption and to carry out a bonding analysis, we calculated the energetics of CO chemisorption on the various surfaces with eH-based methods. It is easier to do a bonding analysis in eH-based methods. The optimized geometries obtained from DFT calculations were used. The BEs calculated by use of eH- and DFT-based methods are reported side by side in Figure 7.

For Pt(111) and $Pt_3Pb(111)$ surfaces, the absolute values for BEs obtained from eH-based calculations are very different from those of DFT-based calculations, but the trend obtained on each surface (Pt(111) and $Pt_3Pb(111)$) is similar for both the methods.

Extended Hückel calculations for the PtPb(0001) surface result in lower BEs compared to those on the other two surfaces, contrary to what is observed in DFT calculations where the binding is somewhat stronger. This underbinding of adsorbates on PtPb(0001) may result from use of eH parameters obtained from the bulk PtPb, where Pt is highly coordinated by Pb (CN = 6) and other Pt atoms (CN = 2). On the PtPb(0001) surface, the Pt atom lies mostly exposed with only one NN Pt and three NN Pb atoms. One of the possible reasons for the underbinding on PtPb(0001) emerges from a detailed bonding analysis, which is discussed in a later section of this paper. Despite the partial disagreement between the eH results and the presumably more reliable DFT results, we feel the many ways available for analyzing the eH wave function make this approach of value.

7. General Characteristics of Chemisorption on a Metal Surface

In order to develop a perspective of small molecule chemisorption (i.e., CO) on intermetallic surfaces, we have to first understand their chemisorption on more common surfaces (i.e., Pt(111)). Here, we take a small digression from our story on intermetallics to look at chemisorption on any surface.

Chemisorption may be thought of as a combination of multiple factors. A polyatomic adsorbing molecule (i.e., CO) not only forms a bond with the surface but also may undergo intramolecular changes that affect both its geometry and

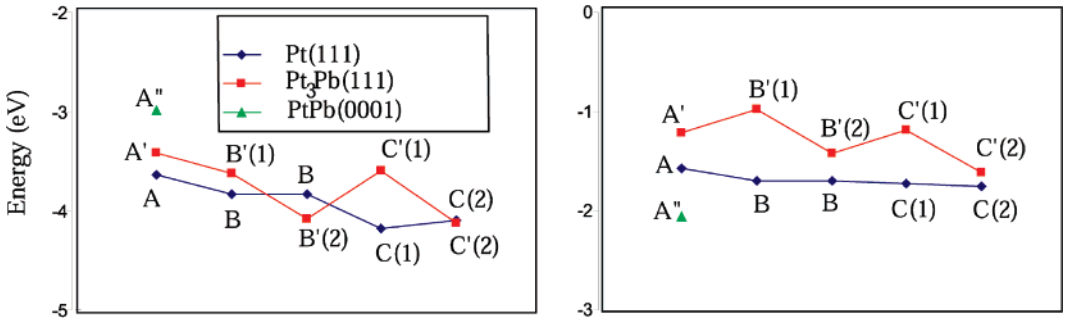

Figure 7. CO binding energies on Pt(111), $Pt_3Pb(111)$, and PtPb(0001) surfaces calculated by use of eH- (left) and DFT-based (right) methods.

energetics. In chemisorption, the surface itself also undergoes some geometric and electronic changes. The overall BE for adsorption of the molecule on the surface is a function of all these factors combined. We use COHP analysis to isolate these contributions to chemisorption and attempt to understand them individually.

In the eH-based COHP analysis, the total energy of any molecule can be divided into a contribution arising from electron occupancy of the valence basis functions (on-site, symbol NS) and contributions arising from interaction of different basis functions (off-site, FS). Thus, the total energy of the molecule can be expressed as

$$E_T = E_{NS} + E_{FS}$$

where E_{NS} = energy contribution from the on-site terms, E_{FS} = energy contribution from the off-site terms, and E_T = total energy of the molecule.

The BE of a molecule on a surface can be expressed as the difference of the total final (E_F) and initial (E_I) energies of the entire surface adsorbate system.

$$BE = E_F - E_I$$

The total final energy of the system can be divided into on-site and off-site terms as

$$E_F = E_{F/NS} + E_{F/FS} + E_{FS/SAB}$$

Here, the first two terms on the right-hand side of the equation refer to the on-site and off-site contributions to the total final energy, respectively. The third term is the off-site term that refers to the surface adsorbate contact (bond) that is formed upon chemisorption of a molecule on the surface (i.e., Pt−CO bond formed due to CO adsorption on Pt(111)). Similarly, the total initial energy can be divided into on-site and off-site terms as

$$E_I = E_{I/NS} + E_{I/FS}$$

The BE can be written as

$$BE = \Delta E_{NS} + \Delta E_{FS} + E_{FS/SAB}$$

where

$$\Delta E_{NS} = E_{F/NS} - E_{I/NS}$$

and

$$\Delta E_{FS} = E_{F/FS} - E_{I/FS}$$

We can, in principle, calculate each of the three terms required to obtain the BE separately

$$\Delta E_{NS} = \sum_{atoms} \Delta e_{NS}$$

and

$$\Delta E_{FS} \approx \sum_{bonds} \Delta e_{FS}$$

where the contribution to the BE from the on-site terms can be evaluated by adding up the differences for on-site terms for various individual atoms (Δe_{NS}). The contribution from the off-site terms can be estimated approximately by adding up the contributions from individual bond interactions (Δe_{FS}) present in the surface slab. The approximation here is that we have neglected the non-nearest neighbor (non-NN) contacts in evaluation of the off-site terms. Localizing the BE to energetic changes in atoms and bonds in the surface and adsorbate will help us trace out various electron movements during the chemisorption event.

There is a further complication arising from the fact that chemisorption brings about concomitant geometric and electronic changes in the surface and the adsorbate. Though the process is artificial, we would like to try to break down the total chemisorption event into energetic contributions from geometric changes in surface and adsorbate and the Pt−CO bond formation. If we imagine that the geometric changes in the surface and adsorbate occur first and then the Pt−CO bond is formed, we can call the former event a "preparation" for bonding. We will develop an estimate of the contribution of this preparation energy in chemisorption.

Also unlike seen in the previous sections, BE differences present at the 3-fold sites (C′(1), C′(2)) of $Pt_3Pb(111)$ are absent at the 3-fold sites (C(1), C(2)) of Pt(111). these sites thus provide us with an interesting case to analyze electron movements in the surface and subsurface layers of a metal and intermetallic surface upon chemisorption.

8. CO Adsorption on the Pt(111) Surface at the hcp Site

First, we investigate CO adsorption on Pt(111) as a model system for small molecule adsorption on surfaces. The surface slab used for eH calculations (same unit cell used in DFT calculations) is shown in section 2 of Supporting Information. The surface slab has four layers and four atoms per unit cell in each layer. The atoms are labeled in Figure 8. Between these atoms there are 21 symmetry distinct bonds, each bond appearing 3 and 6 times. The bonds types are labeled 1−21 in section 3 of Supporting Information. Table 3 describes the Δe_{NS} and Δe_{FS} terms for various atoms and near-neighbor (NN) contacts for CO adsorption at the hcp site of Pt(111) surface.

In the first COHP analysis (Table 4), we show the on-site contributions to the BE for 16 atoms, atom by atom, and the off-site contributions of all 21 bond types, bond by bond. Most change a little upon chemisorption and some a lot. We will look at the overall changes and analyze the major contributions.

The BE obtained from all of the above analysis (addition of terms in the bold font) turns out to be −7.00 eV. This is higher than the actual BE of −4.1 eV. The difference is due to the neglect of the non-NN interaction while estimating the ΔE_{FS} term. Despite the quantitative discrepancy, the analysis provides us a way to dissect the various changes during chemisorption.

As expected, the Pt−CO bond formation is by far the strongest stabilizing influence in CO adsorption (Table 3). The new Pt−C bonds (−32.73 eV) overcome several destabilizing terms: weakening of bonds in the surface (+5.97 eV), weakening of the CO bond (+11.62 eV), and on-site terms that are net destabilizing (+17.41 eV in the Pt surface, not balanced by −9.26 eV in CO).

The destabilizing on-site effects are localized mainly in the top Pt surface layer. The on-site terms from second, third, and fourth layers are all slightly stabilizing.

As for the off-site terms, the overall destabilization is dominated by Pt−Pt bonds forming the 3-fold adsorption site on the top layer (bond type 1). Some subsurface bonds are specifically strengthened (type 3 and 6), as shown in Table 3. The Δe_{FS} surface terms decrease to a negligible value as you get to the third and fourth layers of the slab, as expected.

As mentioned in the earlier section, a part of the overall energetic change may be thought of as being derived from the

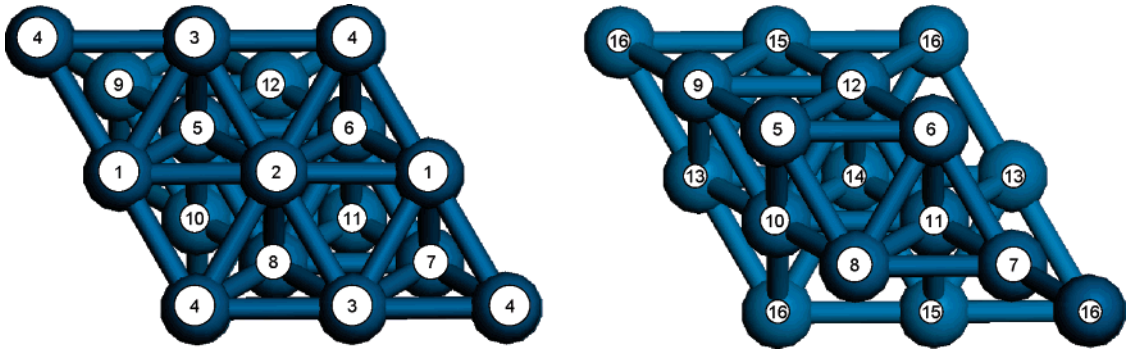

Figure 8. Atoms in the different layers of the Pt(111) slab for CO adsorption at hcp site are labeled. The figure on the left shows the layers one (top), two, and three, and the one on the right shows layers two, three, and four (bottom). CO is bound in the hcp site to atoms 1, 2, and 3 above atom number 5.

TABLE 3: The Contributions to the Binding Energy Term on the Pt(111) Surface Slab Are Shown in an Atom by Atom and Bond by Bond Basis[a]

$\Delta E_{NS} = \sum_{atoms} \Delta e_{NS}$			$\Delta E_{FS} \approx \sum_{bonds} \Delta e_{FS}$		
atom type	atom no.	Δe_{NS}	bond type	no. of bonds of each type	Δe_{FS}
surface atoms			surface bonds		
top layer	1	7.04	1	3	5.37
	2	7.04	2	6	0.30
	3	7.04	3	3	−1.95
	4	1.93	4	3	1.02
second layer	5	−1.07	5	6	0.36
	6	−0.17	6	3	−1.59
	7	−0.17	7	6	0.00
	8	−0.17	8	3	0.00
third layer	9	−1.06	9	3	0.27
	10	−1.06	10	3	0.09
	11	−0.12	11	6	0.72
	12	−1.06	12	3	−0.39
fourth layer	13	−0.21	13	3	0.51
	14	−0.21	14	6	0.30
	15	−0.21	15	3	0.24
	16	−0.13	16	6	0.24
$\sum_{atoms} \Delta e_{NS}$ surface		**17.41**	17	3	0.09
adsorbate atoms			18	3	0.09
C		6.21	19	3	0.12
O		−15.47	20	6	0.06
$\sum_{atoms} \Delta e_{NS}$ adsorbate		**−9.26**	21	3	0.12
			$\sum_{bonds} \Delta e_{FS}$ surface		**5.97**
			adsorbate bonds		
			C−O	1	11.62
			$\sum_{bonds} \Delta e_{FS}$ adsorbate		**11.62**
				$E_{FS/SAB}$	
			surface adsorbate bonds		
			Pt−CO	3	−32.73
			$E_{FS/SAB}$		**−32.73**

[a] The changes to individual terms are large compared to overall BE for the hcp Site. The stabilizing effects essentially originate from the on-site adsorbate term and formation of the surface adsorbate bonds. All other effects are destabilizing.

TABLE 4: $E_{FS/SAB}$ (eV) terms for Chemisorption at the Various Sites on All the Three Surfaces

sites for chemisorption	Pt(111)	Pt_3Pb(111)	PtPb(0001)
top	−24.81	−22.64	−14.45
hcp	−32.73	−30.47	
fcc	−32.54	−31.04	

preparation of geometry of the surface and the adsorbate for chemisorption. The Δe_{NS} and Δe_{FS} terms for this preparation event are shown in section 4 of Supporting Information. A summary of what is observed in the "preparation" is that the only significant contribution arises from stretching the CO bond, which weakens the off-site term (3.15 eV) and strengthens the on-site term (−2.83 eV) on oxygen. The off-site destabilization of the Pt(111) surface slab is 0.31 eV, and the on-site stabilization term is −0.33 eV. Preparation thus plays a minor role in chemisorption. We would neglect this term in further discussions.

The on-site contributions and the weakening and strengthening of bonds are also shown graphically (Figure 9).

Figure 9a graphically shows how the various atoms contribute to the BE through the on-site terms. Red means a positive energy contribution (destabilization) and blue means a negative energy contribution (stabilization). For the Pt(111) surface slab, the Pt atoms that are bound to CO are most destabilized. For the adsorbate C atom, the Δe_{NS} term is positive (destabilizing contribution from the on-site term), and for the adsorbate O atom, the Δe_{NS} term is negative (stabilizing contribution from on-site term). Figure 9b shows the contributions from the off-site terms. Bonds around the adsorption site (hcp, yellow circle)

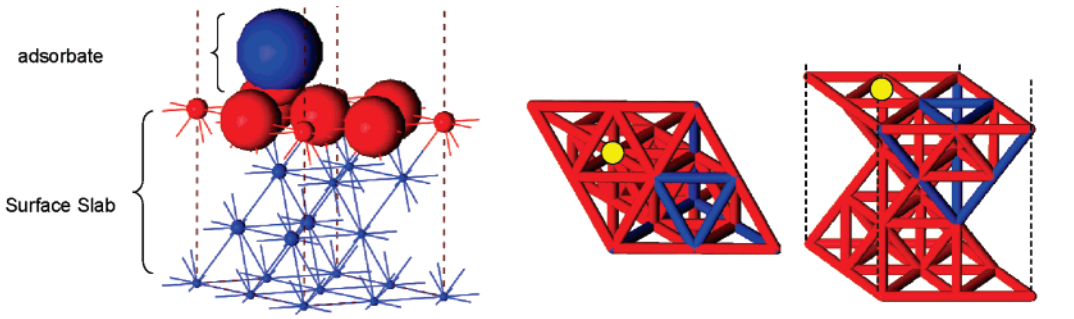

(a) Δe_{NS} term plotted for the Pt(111) surface-slab for CO adsorption at HCP site.

(b) The weakening and strengthening of bonds in the Pt(111) surface-slab for CO adsorption at HCP site.

Figure 9. Graphic representation of the Δe_{NS} term for the Pt(111) surface slab for CO chemisorption at hcp site. (a) A perspective view of the slab with bound CO. The atoms that have a stabilizing influence on the energetics of CO binding are colored blue, and those that have a destabilizing influence are colored red. The volume of the spheres approximates the magnitude of Δe_{NS} stabilization or destabilization. The larger the sphere, the greater is the magnitude of energetic contribution, and vice versa. (b) The bonds in various surface slabs, with red (blue) indicating destabilization (stabilization) of the associated off-site terms contributing to the total energy. The figure on the left in (b) shows the top view of the slab and the one on the right shows the perspective. CO bound on the slab is not shown. The adsorption sites are marked with yellow circles.

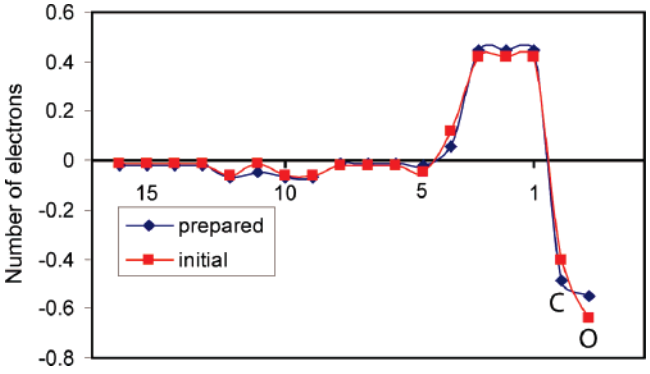

Figure 10. Illustration of the difference in electron densities of each atom of Pt(111) surface slab upon adsorption of CO at hcp site. The red plot shows the electron density changes at various atoms in the surface slab (atoms 1−16, shown in Figure 8 and Table 3) and adsorbate (atoms labeled C and O) when chemisorption of CO occurs at the hcp site of Pt(111). The blue plot corresponds to electron density changes when the initial fragments have been prepared for adsorption by changing the geometry to the final geometry before the Pt−C bond formation. On the *x* axis, the points corresponds to atoms numbered right to left, with the lowest numbers (1−4) representing the top Pt layer and the higher numbers (12−16) representing the bottom layer of the slab (see Figure 8). C and O atoms are labeled separately.

get weakened (red), but those around the other 3-fold site (fcc) get strengthened (blue). The major changes occur around the top layers of the slab. As we go down the layers of the slab, the Δe_{FS} values decrease.

9. Electron Movements in the Pt(111) Surface Slab upon CO Adsorption

We saw a large contribution to the energetic changes coming from the top layer of the surface slab of Pt(111). Next we examine the electron movement in these layers during an adsorption event. Figure 10 shows the difference in the number of electrons at a certain atom (numbered according to Figure 8 and Table 3) with adsorption of CO at the hcp site.

In the Pt(111) surface slab, most of the electron movement occurs in the top layer. The three Pt atoms bound to CO (atoms 1, 2, and 3) lose electrons, as indicated by large positive values of electrons shifted in Figure 10. A CO bound to the surface acquires electron density (approximately one electron per CO molecule) relative to a free CO (as a result of back-donation from Pt to CO). There are some subsurface atoms (5, 9, 10, and 12) that acquire electron density upon chemisorption.

The electron movements parallel the behavior of the Δe_{NS} terms, except in the case of the C atom which tends to have a destabilizing contribution to the chemisorption despite of electron density moving into it. This apparent discrepancy originates from the fact that the Mulliken population analysis (used in "Yet Another extended Hückel Molecular Orbital Package" (YAeHMOP) to calculate charges) accounts for the overlap terms in the Hamiltonian by arbitrarily but systematically sharing the electron density in them equally between the two atoms. One the other hand, in the COHP partitioning analysis, the movement of electrons into overlap regions from the basis function themselves leads to decrease of the on-site and increase of the off-site terms. For example formation of H_2 molecule from two H atoms leads to $\Delta e_{NS} = 7.20$ eV and $\Delta e_{FS} = -12.63$ eV.

In other words, the Mulliken electron density at an atom *i* goes as $c_i^2 + c_i c_j S_{ij}$, where c_i is the atomic coefficient of the molecular orbital and S_{ij} is its overlap with the neighboring atom *j*. As defined, the first term of this density formula is a COHP on-site term, but its second term is classified in the COHP analysis as off site.

The apparent discrepancy at the C atom basically means that the electrons flowing to the C atom from the surface mostly reside in the overlap region (Pt−C). They are thus counted as being a part of electron density at the atom by Mulliken population analysis but not by the on-site terms.

We already mentioned that it is also possible to think of chemisorption in stages, constructing a "prepared" surface and CO and then interacting them. The dark blue curve in Figure 10 shows the electron movements between a prepared surface and prepared CO. The electron movements occurring when the geometrical preparation of Pt(111) slab and CO molecule for adsorption are an order of magnitude less than the electron movements upon Pt−C bond formation. The minimal difference between the curves shows that the majority of the electron movements occur during the Pt−C bond formation event, a fact consistent with earlier energy partitioning calculations (Table 3 in this paper and section 4 in the Supporting Information).

10. Investigating Binding Energy Trends Using Extended Hückel-Based Calculations

The two important trends we had noticed in the eH-based BE calculations on these surfaces (Figure 7) are as follows:

1. $Pt_3Pb(111)$ has a lower binding energy for CO chemisorption than Pt(111) in general, and PtPb(0001) has the lowest binding energy. This can be seen clearly in chemisorption at the Pt-top sites on these surfaces.

2. The binding energies on the $Pt_3Pb(111)$ vary with the chemisorption site compared to those on the Pt(111) surface. The former binding energies jump to higher values whenever there is a Pb atom underneath the adsorption site (seen best at the 3-fold sites C(1), C(2) on Pt(111) and C′(1) and C′(2) on $Pt_3Pb(111)$).

Regrettably, the first conclusion is in disagreement with the DFT result that the binding energy of CO to PtPb(0001) seems to be higher than that on the other two surfaces. We have no experimental work to guide us as to which result to believe. We chose to analyze the eH result, in the process gaining a hint as to the possible disagreement between the methods.

From a previous section, we have learned that the $E_{FS/SAB}$ term (surface adsorbate bond formation) is the strongest and the most stabilizing interaction upon chemisorption. So in order to further investigate the trends on these surfaces, we focus on this term. It is shown in Table 4 for the top and the 3-fold chemisorption site on all these surfaces.

We see that the first trend can be explained well by use of only the $E_{FS/SAB}$ term. At the top sites, this term is strongest on Pt(111) and weakens as we move to $Pt_3Pb(111)$ and even more as one moves to PtPb(0001) surface.

We do not have an obvious explanation of the second trend from the $E_{FS/SAB}$ values at the 3-fold sites. The $E_{FS/SAB}$ term for $Pt_3Pb(111)$ is weaker than that for Pt(111), as indicated by the first trend.

This makes us think that the variation in binding energies on $Pt_3Pb(111)$ originates not from the Pt−C bonding but from some other term in the chemisorption event. So, in order to understand the second trend, we have to dive deeper into the analysis of the electronic effects of chemisorption. In the next section, we do a full COHP analysis of the CO chemisorption on Pt(111) and $Pt_3Pb(111)$ 3-fold sites. The first trend is studied in a later section of this paper (section 13).

11. CO Adsorption on the Pt(111) (fcc Site) and Pt_3Pb-(111) (hcp, fcc Sites) Surfaces

As we have already carried out a detailed analysis of chemisorption at the hcp site on the Pt(111) surface, we focus here on the remaining 3-fold sites on Pt(111) and $Pt_3Pb(111)$. We have carried out similar analyses by use of energy partitioning and electron movements for chemisorption at the other 3-fold site (fcc) of Pt(111) and both 3-fold sites of Pt_3-Pb(111). The detailed numbers are given in sections 5, 6, and 7 of Supporting Information. In order to get at the essentials and free ourselves from the relatively tedious (and changing) numbering of atoms and bonds in various surface slabs, we have illustrated the on-site Δe_{NS} terms graphically in Figure 11a,c,e. Bonds that get strengthened (blue) and weakened (red) for all the surface slabs are also shown (Figure 11b,d,f). The degree of bond weakening/strengthening is not in the figure but can be inferred from sections 5, 6, and 7 of the Supporting Information.

As for the chemisorption at the hcp site of Pt(111), we find for the fcc site that the top layer is highly destabilizing through its on-site terms, an effect counteracted to a small degree by the layers below (Figure 11). There are differences but the overall effect is quite similar for adsorption at both hcp and fcc sites. This is reflected in the very similar BEs at the two sites.

In the $Pt_3Pb(111)$ surface slab, the Δe_{NS} terms are destabilizing for most atoms. The atoms in the top layers typically get greatly destabilized, as in case of Pt(111) surface. There is a small stabilizing contribution arising from the Pb atom in the second layer. The off-site terms provide both stabilizing and destabilizing contributions. The difference from Pt(111) surface slab comes about through the stabilizing interactions penetrating deeper in the $Pt_3Pb(111)$ surface slab.

The noticeable difference between chemisorption at the hcp and fcc sites on $Pt_3Pb(111)$ comes about through the difference in the size of the on-site terms. Both the third and the fourth layers of $Pt_3Pb(111)$ slab contribute substantially to destabilization of the surface slab in the case of hcp adsorption. The on-site terms for adsorption at an fcc site are much smaller. This does not happen in the Pt(111) surface slab, hinting at different electron drifts in Pt(111) and $Pt_3Pb(111)$ surface slabs.

12. Comparison of Electron Movements in the Pt(111) and $Pt_3Pb(111)$ Surface Slabs

Electron movements (from Mulliken population analysis) for adsorption of CO at both Pt(111) and $Pt_3Pb(111)$ surfaces at various 3-fold sites are shown in Figure 12 (compare earlier Figure 10). The difference plots between the adsorption at fcc and hcp sites are indicated in green.

The electron movements usually get reflected in the Δe_{NS} terms. In the Pt(111) surface, most of the electron movements occur in the top layer. The difference in the electron movements between fcc and hcp adsorption is minimal, reflected in very similar BEs for hcp and fcc sites on Pt(111).

For the $Pt_3Pb(111)$ surface, the difference in the electron movements following chemisorption at the hcp and fcc sites is much more pronounced. The top surface layers lose electrons and the CO molecule gains electrons, as on Pt(111), but the amount of electron removal from the top layer is different for chemisorption at hcp and fcc sites. In the case of chemisorption at the fcc site, the top Pt atoms tend to lose more electrons than in the case of chemisorption at the hcp site. The C atom of CO receives more electrons on hcp chemisorption than what happens when the chemisorption is at the fcc site on Pt_3Pb-(111). A difference in electron movements also occurs in the third and fourth layers of the slab (something also reflected in the Δe_{NS} terms discussed in the earlier section). The consequence is a difference (see green line) in electron movement upon chemisorption. This is connected to the different BEs for CO at hcp and fcc sites of $Pt_3Pb(111)$.

Concerned at that distant effect (the third and fourth layer electron movements), we carried out similar calculations for $Pt_3Pb(111)$ slabs made out of five layers. The BE difference between the hcp and fcc chemisorption remained the same. The electron movements occurring in the adsorbate and the top three layers of the slab were preserved. The electron movements in the bottom layer of surface slab in hcp adsorption also remain in the bottom layer of the five-layer slab. The effects of hcp chemisorption seem to penetrate deeper than those of fcc chemisorption, to the end of the slab (both four- and five-layer slabs). We remain uncertain whether some part of this phenomenon may be an artifact of the finite slab widths we choose to simulate semi-infinite surfaces in our calculations.

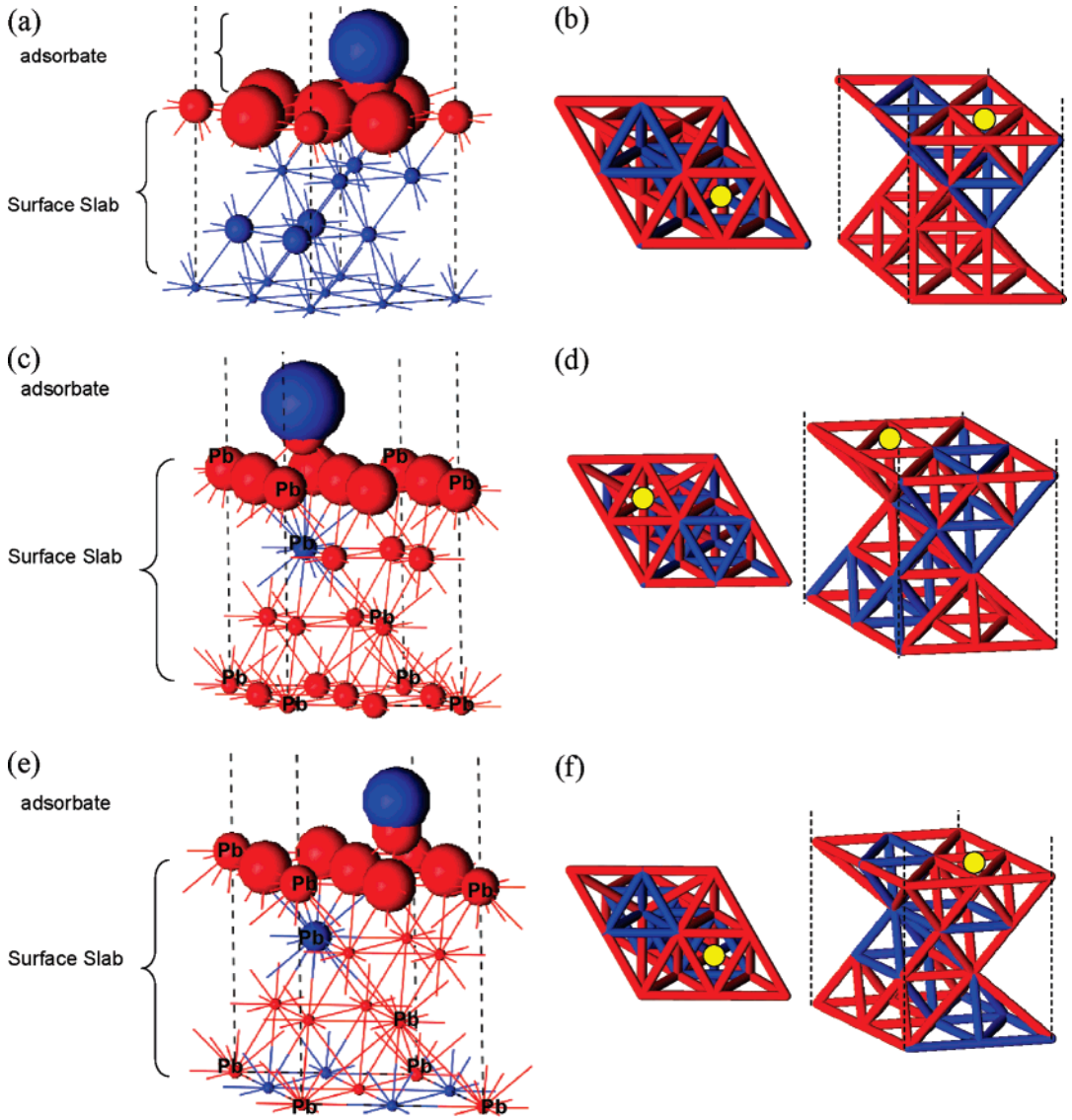

Figure 11. A graphic representation of the on-site Δe_{NS} terms for various surface slabs (a, c, and e). The atoms that have a stabilizing influence (through Δe_{NS}) on the energetics of CO binding are colored blue, and those that have a destabilizing influence are colored red. The volume of the spheres approximates the magnitude of stabilization or destabilization. The larger the sphere, the greater in magnitude is the energetic contribution, and vice versa. The bonds in various surface slabs are shown (b, d, and f). The figure on left shows the top view of the slab, while the one on right shows a perspective. The bonds colored red are the ones that get weakened (off-site terms) upon CO chemisorption. The bonds colored blue get strengthened upon CO chemisorption. The adsorption sites are marked with yellow circles. (a) Δe_{NS} term plotted for the Pt(111) surface slab for CO adsorption at fcc site. (b) The weakening and strengthening of bonds in the Pt(111) surface slab for CO adsorption at fcc site. (c) Δe_{NS} term plotted for the $Pt_3Pb(111)$ surface slab for CO adsorption at hcp site. Pb atoms are labeled. (d) The weakening and strengthening of bonds in the $Pt_3Pb(111)$ surface slab for CO adsorption at hcp site. (e) Δe_{NS} term plotted for the $Pt_3Pb(111)$ surface slab for CO adsorption at fcc site. Pb atoms are labeled. (f) The weakening and strengthening of bonds in the $Pt_3Pb(111)$ surface slab for CO adsorption at fcc site.

13. Pt−CO Interaction at the Top Site on Various Surfaces

As seen in the earlier sections, the $E_{FS/SAB}$ term that describes Pt−CO bonding is the dominant term in chemisorption. This term is also consistent (within the eH results) with the first trend in binding energies mentioned in section 10. We devote this section to further investigation of this trend (mentioned in section 11) with the $E_{FS/SAB}$ term. We study this term for the top site adsorption of CO on all the three surfaces; a Frontier Molecular Orbital (FMO) analysis of the chemisorption is helpful in this regard.

Although the BE trend obtained by use of eH at the top site disagrees with the DFT results for PtPb(0001), we go further and analyze the trend even on PtPb(0001) in the perspective of what happens on Pt(111) and $Pt_3Pb(111)$.

Figure 13 shows the partial density of states (PDOS) for the orbitals of chemisorbed CO on a Pt(111) surface. Four orbitals (4σ, 5σ, and two 2π orbitals) of CO interact significantly with the surface Pt atom; their occupancies are then significantly modified relative to a free CO molecule. 4σ and 5σ have more of a C−O nonbonding character to them, whereas the 2π orbitals are C−O antibonding. Other orbitals (3σ, π, and 6σ) are either completely filled or completely empty with no difference in electron occupancy from free CO, in effect not entering interaction.[28] The $Pt_3Pb(111)$ and PtPb(0001) surface chemisorptions are similar. From a frontier orbital perspective, this is what one would expect; 5σ and 2π orbitals are close to the Fermi energy.

The interactions of these CO orbitals with the surface Pt atom have been evaluated with the COHP technique. The integration

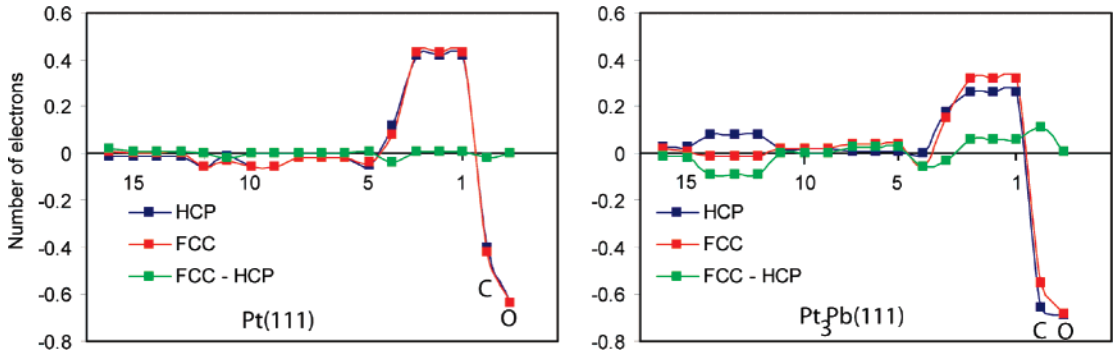

Figure 12. The difference in electron densities of each atom type of the Pt(111) and $Pt_3Pb(111)$ surface slabs upon adsorption of CO at the hcp and fcc sites. The *x* axis numbers the atoms right to left (see sections 5, 6, and 7 of Supporting Information for numbering of atoms in Pt(111) and $Pt_3Pb(111)$ surface slabs at the hcp and fcc sites), with the lowest numbers (1−4) representing the top layer and the higher numbers (12−16) representing the bottom layer of the slabs. C and O atoms are labeled separately. The difference plots between chemisorption at fcc and hcp adsorption are shown in green.

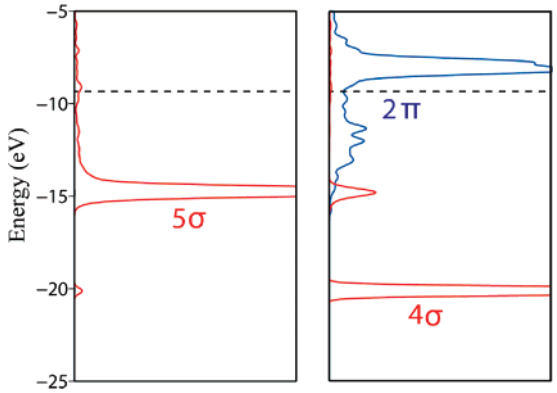

Figure 13. The PDOS for various molecular orbitals of CO (4σ, 5σ, and 2π, those that interact significantly with Pt surface) chemisorbed at the top site on Pt(111) surface. Various CO orbitals are labeled in color and separated into two panels for clarity. The Fermi energy is shown with dashed lines.

TABLE 5: Integrated COHP Values for Orbital Interactions between CO (adsorbed at the Top Site) and the Surface Pt Atom

interactions	Pt(111)	$Pt_3Pb(111)$	PtPb(0001)
4σ−d(Pt)	−0.88	−0.47	−0.89
4σ−s(Pt)	−2.24	−2.09	−2.16
4σ−p(Pt)	−1.99	−2.30	−1.55
5σ−d(Pt)	−2.42	−1.87	−2.05
5σ−s(Pt)	−3.52	−3.41	−2.90
5σ−p(Pt)	−2.23	−3.72	−3.03
2π−d(Pt)	−8.78	−6.82	1.29
2π−s(Pt)	0.00	0.00	0.00
2π−p(Pt)	−1.09	−1.56	−3.03

of COHP values up to the Fermi energy is reported in Table 5. Details of the COHP calculations are given in sections 8, 9, and 10 of the Supporting Information. Although the eH binding energies on the PtPb(0001) surface shift in opposite directions relative to binding energies on Pt(111) and $Pt_3Pb(111)$ when compared with DFT results, we believe that the FMO analysis would be still helpful in understanding the Pt−CO interaction on PtPb(0001). We have looked into the Pt−CO interaction on PtPb(0001) surface in light of what happens on the Pt(111) and $Pt_3Pb(111)$ surfaces.

If we sum up all the interactions on one surface, we can see the trends in binding energy obtained from eH calculations. The interactions add up to −23.15 on Pt(111), −22.24 on $Pt_3Pb(111)$, and −14.32 on PtPb(0001).

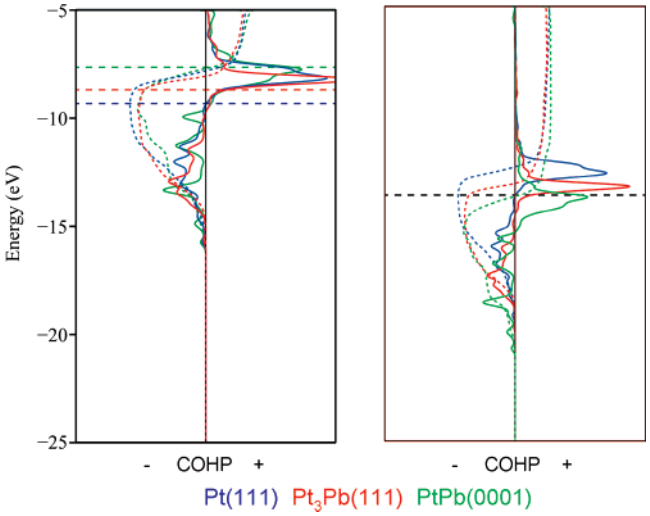

Figure 14. COHP curves (including integrated COHP in colored dashed lines) for CO 2π interactions with surface Pt d orbitals on various surfaces (labeled in color). In the left figure, all surfaces are shown on the same energy scale. The Fermi energy (labeled with horizontal dashed lines) increases with increasing atomic percentage of Pb. The antibonding region of d(Pt)−2π(CO) gets increasingly filled up with increasing Fermi energy. The figure at right shows the same results in a different way; here, all the Fermi energies are fixed at the same level. The different values for integrated COHP (iCOHP) curves at the Fermi energy can be clearly seen.

Although there are significant variations in 4σ and 5σ orbital interactions between Pt−CO, Table 5 clearly shows the determining role (and the difference between PtPb(0001) and other surfaces) of the d(Pt)−2π(CO) interaction. Effects of moving from Pt toward Pb-containing intermetallics for all the interactions are discussed in detail in the Supporting Information.

2π(CO)−d(Pt) interactions (Figure 14, the same result presented in two different ways) contribute most to bonding or attractive Pt−CO interactions on Pt(111) and $Pt_3Pb(111)$ surfaces. But the analogous interactions are net repulsive on PtPb(0001). Let us see if we can understand this striking difference.

As noted above, the 2π(CO)−d(Pt) interaction is strong. The lower-lying Pt d levels mix into themselves CO 2π in a Pt−CO bonding way, while the upper-lying CO 2π levels mix in Pt d levels in an antibonding way. On Pt(111), it is mainly the metal d band that is filled. This leads to filling of 2π(CO)−d(Pt) bonding levels only.

TABLE 6: Occupation of Surface Pt Bands on Clean Surfaces

number and type of bands of the surface Pt atom	Number of electrons in the orbitals		
	Pt(111)	Pt_3Pb(111)	PtPb(0001)
d (5)	8.91	9.11	9.26
s (1)	0.36	0.35	0.48
p (3)	0.19	0.21	0.58

On moving from Pt(111) to the Pb-containing intermetallic surfaces, the electron filling increases (seen clearly in Figure 14 (left)). In Pt_3Pb(111), the Fermi level rises slightly. This leads to filling of some of the 2π(CO)−d(Pt) antibonding levels, leading in turn to weakening of this stabilizing interaction. This can be seen in the smaller negative integrated COHP (iCOHP) value at the Fermi level for Pt_3Pb(111) compared to that for Pt(111) (Figure 14 (right)), and the same factor may be responsible for the lower CO binding energies calculated on Pt_3Pb(111) compared to those on Pt(111) (Figure 7). With PtPb-(0001), the Fermi level moves even higher in energy. As Figure 14 shows, a large number of 2π(CO)−d(Pt) antibonding levels are filled. The 2π(CO)−d(Pt) interaction becomes net repulsive.

In order to learn more about the effect of the increasing Fermi level, we calculated the occupancies of various levels at the surface Pt atoms on all the three surfaces before chemisorption (Table 6). On going from Pt(111) to Pt_3Pb(111), the s and p band filling remains about the same. It is the Pt d band occupancy that increases noticeably (8.91 to 9.11). This is likely to be a combined result of smaller Pt d bandwidth (compared to Pt s and p) and additional electrons that are transferred from the Pb atoms. On further moving to PtPb(0001), we see that band occupancies of all the Pt levels increase.

The total electron counts of surface Pt atoms in the cases of Pt(111) (9.47 electrons) and Pt_3Pb(111) (9.67 electrons) reveal that the Pt atoms are positively charged (relative to a free atom), whereas the surface Pt atom on PtPb(0001) is negatively charged (10.32 electrons).

Where does this change in surface Pt atom population come from? Figure 3 (in the beginning section) shows the PDOS for Pt and Pb atoms in all the three solids. For Pt, there are four atoms (40 electrons) per unit cell. Due to the overlap in energy of the lower part of the wide Pt s and p bands with the narrow Pt d band some electrons are transferred from the Pt d to the Pt s and p, resulting in partial occupancy of Pt d.

For Pt_3Pb, with 3 Pt atoms and 1 Pb atom per unit cell, there are 34 ($3 \times 10 + 4$) electrons per unit cell. Out of these, approximately two Pb electrons stay in Pb s orbitals, much lower in energy than Pt orbitals; the 2 Pb p electrons interact and mix with Pt orbitals. With that electron sharing comes electron transfer from Pb to Pt. The narrower Pt d band also contributes.

PtPb has 2 Pt and 2 Pb atoms in the unit cell with an electron count of 28 ($2 \times 10 + 2 \times 4$). Four electrons remain in two Pb s orbitals far down in energy. Four electrons in Pb p orbitals are available for donation to Pt orbitals. Here, the Pt d band is even narrower than that for Pt_3Pb; the electron donation from Pb increases the electron count on the Pt atoms.

In these, electron donations may be found as a clue to the explanation of the discrepancy in trend between the eH and DFT binding energies with respect to binding energy on PtPb(0001) (which is much weaker than the other two surfaces). Whereas the Pt(111) and Pt_3Pb(111) surfaces are positively charged, there is a substantial negative charge on the top Pt atoms on PtPb-(0001). This negative charge on the surface Pt of PtPb(0001) may result in substantial shifting of electronic levels compared to those on the other two surfaces, an effect that is not captured in the eH formalism. In turn, this may contribute to the discrepancy between the binding energies obtained from DFT and eH calculations for PtPb(0001).

In addition to our main goal of understanding chemisorption on intermetallic surfaces, we also wanted to understand the resistance to CO poisoning of PtPb in formic acid. From our calculations on pristine surfaces (both DFT and extended Hückel), we can definitely rule out the possibility that CO does not bind to a pristine PtPb surface (CO binds well). The FMO analysis with eH calculations indicates that the Pt−CO is weakened as the atomic percent of Pb increases, but the DFT binding energies on PtPb(0001) do not follow this trend and in fact show a higher chemisorption energy for CO on PtPb(0001) than those on the Pt(111) and Pt_3Pb(111) surfaces. It is also likely that the electrochemical environment plays a role in the experimentally observed behavior, the effects of which are not considered here. Future studies (both theoretical and experimental) in the electrochemical environment should provide us more clues about the absence of CO poisoning on PtPb surfaces.

14. Conclusions

Electronic structure calculations for CO and H adsorption on Pt(111), Pt_3Pb(111), and PtPb(0001) surfaces reveal several trends. The binding energies on Pt_3Pb(111) are in general lower than those on Pt(111). The binding energies on PtPb(0001) show a discrepancy between DFT and eH results. DFT results indicate that PtPb(0001) surface has higher binding energy than the other two surfaces, and eH results indicate the opposite. Besides, the presence of Pb in the subsurface layer under the chemisorption site on Pt_3Pb(111) leads to stronger binding at the 2- and 3-fold sites compared to those at sites that do not have a Pb atom underneath.

We analyzed the electronic effects of chemisorption in detail, looking at changes happening in the surface and in the adsorbate. The results indicate that the electronic effects of chemisorption penetrate deep into the surface slabs. The compositions of subsurface layers are important in determining the BEs of the adsorbates.

The large size of the $E_{FS/SAB}$ term indicates that Pt−adsorbate bond formation is the most significant term in chemisorption. These off-site terms can explain the general trend of decreasing binding energies with increasing percentage of Pb atoms in these intermetallics.

To explain the second trend (that the binding energy varies considerably with the choice of the 2- and 3-fold sites on Pt_3-Pb(111) compared to the corresponding Pt(111)), we have carried out a detailed COHP-based analysis on the surface and adsorbate. The results indicate that electron drifts upon chemisorption at two different 3-fold sites on Pt_3Pb(111) surface are different, while they are similar in chemisorption on the Pt-(111) surface. This difference eventually manifests itself in different BEs for hcp and fcc sites on Pt_3Pb(111).

Returning to the first trend (that binding on Pt is stronger than on Pt−Pb intermetallics), we have further studied in detail the $E_{FS/SAB}$ terms (Pt−CO bonding) by use of an FMO analysis. Here, we have included eH results on the PtPb(0001) surface in our analysis, despite a discrepancy with the DFT results. Higher band filling of surface Pt orbitals with higher Pb content seems to be the important factor that influences Pt−CO interaction as we move from Pt to the Pb-containing intermetallics.

TABLE 7: Extended Hückel Parameters Used for Calculations in This Paper

orbitals	H_{ii}	c1	exponent 1	c2	exponent 2
Pt					
6s	−9.077		2.554		
6p	−5.475		2.554		
5d	−12.590	0.67186	6.013	0.5847	2.200
Pb					
6s	−15.700		2.600		
6p	−8.000		2.060		
C					
2s	−21.400		1.625		
2p	−11.400		1.625		
O					
2s	−32.300		2.275		
2p	−14.800		2.275		

15. Appendix

Extended Hückel Parameters Used in the Calculations. The eH parameters used are shown in Table 7. The default values of the extended Hückel parameters implemented in the YAeHMOP program are not meant to model extended systems such as solids and surfaces. We adjusted the parameters, fitting band structures obtained from plane-wave DFT calculations on the bulk structures. Specifically, Pt d basis functions have been made more diffuse (compared to the default parameters) to match the larger band widths obtained from the DFT calculations.

Acknowledgment. We thank Peter Kroll for various discussions on DFT calculations. We thank the Ohio Supercomputing Center for computing time and the Department of Energy (Grant No. DE-FG02-03ER46072) for supporting this project.

Supporting Information Available: (1) Surface unit cell of Pt(111) used for eH calculations, (2) Pt−Pt contacts for Pt(111) surface slab labeled, (3) H-atom chemisorption, (4) estimation of contribution to the overall energetics of chemisorption from geometrical changes to the surface and the adsorbate, (5) the contributions to the binding energy calculated for CO adsorption at fcc site on Pt(111), (6) the contributions to the binding energy calculated for CO adsorption at hcp site on $Pt_3Pb(111)$, (7) the contributions to the binding energy calculated for CO adsorption at fcc site on $Pt_3Pb(111)$, (8) CO interaction with a surface Pt atom on Pt(111), (9) CO interaction with a surface Pt atom on $Pt_3Pb(111)$, (10) CO interaction with a surface Pt atom on PtPb(0001), and (11) Pt−CO interaction and the electron filling for surface Pt orbitals. This material is available free of charge via the Internet at http://pubs.acs.org.

References and Notes

(1) Lamy, C. L.; Jean-Michel, L.; Srinivasan, S. *Direct Methanol Fuel Cells: from a Twentieth Century Electrochemists Dream to a Twenty-First Century Emerging Technology*; Kluwer Academic/Plenum: New York, 2001; Vol. 34.

(2) Casado-Rivera, E.; Volpe, D. J.; Alden, L.; Lind, C.; Downie, C.; Vazquez-Alvarez, T.; Angelo, A. C. D.; DiSalvo, F. J.; Abruna, H. D. *J. Am. Chem. Soc.* **2004**, *126*, 4043.

(3) Gasteiger, H. A.; Markovic, N.; Ross, P. N.; Cairns, E. J. *J. Phys. Chem.* **1994**, *98*, 617.

(4) Gasteiger, H. A.; Markovic, N. M.; Ross, P. N. *J. Phys. Chem.* **1995**, *99*, 8290.

(5) Hoffmann, R. *J. Chem. Phys.* **1964**, *40*, 2745.

(6) Hoffmann, R. *J. Chem. Phys.* **1964**, *40*, 2480.

(7) Hoffmann, R. *J. Chem. Phys.* **1964**, *40*, 2474.

(8) Hoffmann, R. *J. Chem. Phys.* **1963**, *39*, 1397.

(9) Perdew, J. P.; Chevary, J. A.; Vosko, S. H.; Jackson, K. A.; Pederson, M. R.; Singh, D. J.; Fiolhais, C. *Phys. Rev. B* **1992**, *46*, 6671.

(10) Perdew, J. P.; Chevary, J. A.; Vosko, S. H.; Jackson, K. A.; Pederson, M. R.; Singh, D. J.; Fiolhais, C. *Phys. Rev. B* **1993**, *48*, 4978.

(11) Perdew, J. P.; Burke, K.; Ernzerhof, M. *Phys. Rev. Lett.* **1996**, *77*, 3865.

(12) Perdew, J. P.; Burke, K.; Ernzerhof, M. *Phys. Rev. Lett.* **1997**, *78*, 1396.

(13) Kresse, G.; Hafner, J. *Phys. Rev. B* **1993**, *47*, 558.

(14) Kresse, G.; Hafner, J. *Phys. Rev. B* **1994**, *49*, 14251.

(15) Kresse, G.; Hafner, J. *J. Phys.: Condens. Matter* **1994**, *6*, 8245.

(16) Kresse, G.; Furthmüller, J. *Comput. Mater. Sci.* **1996**, *6*, 15.

(17) Kresse, G.; Furthmüller, J. *Phys. Rev. B* **1996**, *54*, 11169.

(18) Kresse, G.; Joubert, D. *Phys. Rev. B* **1999**, *59*, 1758.

(19) Dronskowski, R.; Bloechl, P. E. *J. Phys. Chem.* **1993**, *97*, 8617.

(20) Glassey, W. V.; Papoian, G. A.; Hoffmann, R. *J. Chem. Phys.* **1999**, *111*, 893.

(21) Hoffmann, R. *Solids and surfaces: a chemist's view of bonding in extended structures*; WILEY-VCH: New York, 1988.

(22) Monkhorst, H. J.; Pack, J. D. *Phys. Rev. B* **1976**, *13*, 5188−5192.

(23) Yeo, Y. Y.; Vattuone, L.; King, D. A. *J. Chem. Phys.* **1997**, *106*, 392.

(24) Lynch, M.; Hu, P. *Surf. Sci.* **2000**, *458*, 1.

(25) Ogletree, D. F.; Van Hove, M. A.; Somorjai, G. A. *Surf. Sci.* **1986**, *173*, 351.

(26) Olsen, R. A.; Philipsen, P. H. T.; Baerends, E. J. *J. Chem. Phys.* **2003**, *119*, 4522.

(27) Shubina, T. E.; Koper, M. T. M. *Electrochim. Acta* **2002**, *47*, 3621.

(28) Sung, S. S.; Hoffmann, R. *J. Am. Chem. Soc.* **1985**, *107*, 578.